Design Trade-offs for Airborne Phased Array Radar for Atmospheric Research

Jorge L. Salazar, Eric Loew, Pei-Sang Tsai,
Jothiram Vivekanandan and Wen Chau Lee
National Center for Atmospheric Research (NCAR)
3450 Mitchell Lane Boulder, CO 80301, USA

V. Chandrasekar
Colorado State University (CSU)
NCAR Affiliate Scientist
1373 Fort Collins, CO 80523, U

Abstract **-** This paper discusses the design options and trade-offs of the key performance parameters, technology, and costs of dual-polarized and two-dimensional active phased array antenna for an atmospheric airborne radar system. The design proposed provides high-resolution measurements of the air motion and rainfall characteristics of very large storms that are difficult to observe with a ground-based radar system. Parameters such as antenna size, wavelength, beamwidth, transmit power, spatial resolution, along-track resolution, and polarization have been evaluated. The paper presents a performance evaluation of the radar system. Preliminary results from the antenna front-end section that corresponds to a Line Replacement Unit (LRU) are presented.

Index Terms – Airborne Doppler radar, ELDORA, phased array radar, dual-polarized.

I. Introduction

The National Center for Atmospheric Research (NCAR) has investigated several potential phased array radar configurations for a next-generation airborne research radar for atmospheric observations [1]. The proposed Airborne Phased Array Radar (APAR) is conceived as replacing the X-band Electra Doppler radar (ELDORA) with improvements such as higher radar sensitivity, better along-track resolution and hydrometeor classification using dual polarization [2]. ELDORA Doppler radar was implemented with two single-polarized slotted waveguide array antennas to generate two beams separated by ~40º (fore and aft) beams. A fast mechanical rotating radome (rotodome) was attached to the modified tail of the aircraft to produce a scanning rate of 144 deg/sec; a step-chirped waveform was implemented to enhance the along-track resolution to 300 m.

During the past 10 years, two U.S. Navy surveillance phased-array radars have been modified for use as weather radars. The first one is the National Weather Radar Testbed (NWRT) operated by the NOAA National Storm Severe Laboratory (NSSL) [4] and the second is the Mobile Weather Radar, 2005 X-Band, Phased Array (MWR-05XP) operated by Processing [5].

Besides the fact that both are single-polarized and passive arrays, fast electronically scanned beams have provided the scientific community with higher temporal resolution measurements that improve detection and warning for severe high-impact weather. Tornado false alarm rates have been reduced substantially and the tornado warning lead times extended from 14 minutes to 20 minutes [4].

Considering the benefit of phased array technology, academic, state, federal, and private institutions have been working together to develop phased-array radar for atmospheric applications. Currently, the Massachusetts Institute of Technology's Lincoln Laboratory (MIT-LL) is developing a multifunction, two-dimensional (2-D), dual-pol, flat and multifunction S-band radar system [6]. One of the biggest challenges in this development is achieving acceptable polarization performance [7]. In order to overcome this constraint, the National Severe Storm Laboratory (NSLL) and University of Oklahoma are evaluating the possibility of prototyping a Cylindrical Polarimetric Phased-Array Radar (CPPAR) for practical scan-invariant weather measurements [8]. Another approach proposed by the Center for Collaborative Adaptive Sensing of the Atmosphere (CASA) [9], consists of a low-power, low-cost dual-polarized phased array radar. To overcome polarization distortion, the CASA radar performs the electronic scan only in the principal planes where cross-polarization isolation is relatively easy to obtain [9].

The design of the NCAR Airborne Phased Array Radar (APAR) envisions it being flown on the NSF/NCAR C-130. It would consist of four distinct dual-polarized and 2-D scanning active phased array antennas, strategically located about the fuselage. The C-130 aircraft is the airborne platform for atmospheric observations, which facilitate real state and prime power for the installation of four active electronically scanned array antenna panels. The C-130 aircraft also includes atmospheric instruments such as dropsondes and other standard thermodynamic, microphysics, and radiation sensors for sampling and remote sensing of clouds, chemistry, and aerosols [3].

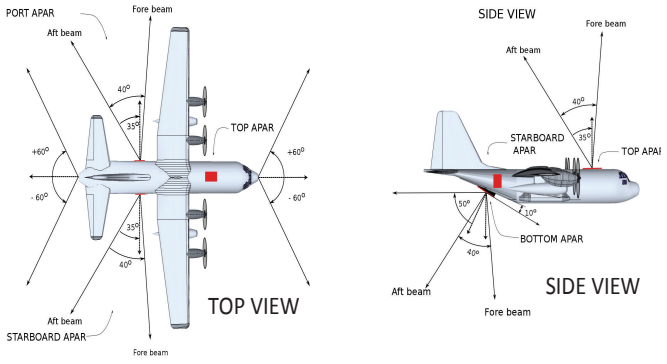

a) b)

Fig. 1. Representation of the four phased-array radars on the NSF/NCAR C130 turboprop aircraft. a) Side view and b) Top view.

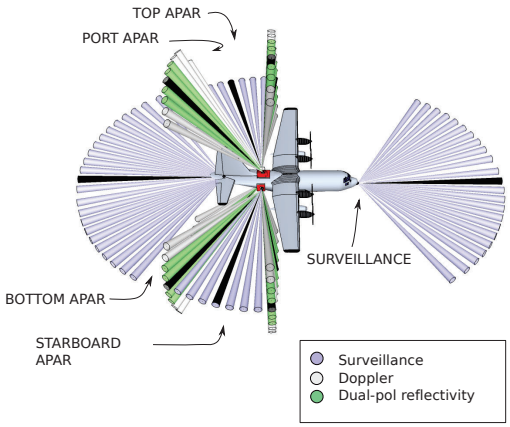

Fig. 2. Representation of the phased-array radars on the NSF/NCAR C130 turboprop aircraft and scanning radar modes (surveillance, Doppler and dual-pol reflectivity).

II. AIRBORNE RADAR DESCRIPTION

The proposed APAR system consists of four C-band active electronically scanned array (AESA) antennas strategically mounted on the fuselage of the NSF/NCAR C-130 aircraft. One AESA will be mounted on each side of the fuselage behind the rear doors; the third will be mounted on the top of the fuselage and the fourth on the upper portion of the tail ramp, as shown in Figure 1.

The AESAs will be operated primarily in two modes: dual-Doppler and surveillance. Dual-Doppler mode will be the primary mode of operation. In this mode, each of the four AESAs will generate a single "pencil" beam that will scan in azimuth and elevation. Scanning in azimuth will be between two fixed angles, one fore and one aft, separated by approximately 40°. Given the proposed configuration on the C-130, the fore and aft azimuth angles will not be symmetrical around 0 ° (normal to the fuselage) as is the case for the present ELDORA system, which is likely to be +5°/-35°. Scanning will be done to maximize the number of independent samples while covering the desired spatial domain (±50° in elevation) in the least amount of time. The "composite" scanning of all four AESAs yields a 360°, dual-Doppler coverage, as in the current ELDORA [3]. It is worth mentioning that the dual-polarization data will only be collected on the fore beams and within ± 20^0 elevation angles to ensure the best quality of the dual-polarization data [13]. A composite surveillance scan, consisting of the bottom and side AESAs as shown in Figure 2 will also be performed periodically to establish situational awareness.

Each AESA is designed to operate at 5.4 GHz and the size of the aperture fits the maximum aperture available in the C130 fuselage (1.6 m x 1.9 m). A planar array with a spacing square grid of 0.5 λ_o is composed of 3,584 active radiating elements, arranged in a rectangular array of 56 line replace units (LRUs). Each LRU is composed of 64 (8x8) radiating elements. Figure 3 shows a simplified block diagram of an APAR.

It consists of six components: (1) the RF array antenna front end, (2) quad T/R modules, (3) array antenna backplane, (4) radar digital backend, (5) radar processor/display, and (6) radar scheduler. Components 1-3 reside outside the fuselage enclosed by fairings and present the greatest technical challenge. NCAR is currently working with MIT\LL to develop a quad T/R module. NCAR is developing the RF array front end and array antenna backplane (components 1 and 3) for an LRU. Table 2 presents a summary of the characteristics of proposed APAR system.

III. RADAR DESIGN TRADE-OFFS

The radar development involves consideration of the radar sensitivity, sampling, spatial and along track resolution.

A. *Physical constraints: Aperture size and weight.*

The NSF/NCAR C-130 turboprop fuselage provides an available area (1.9 m x 1.6m) for each aperture array antenna. A maximum weigh of about 600 pounds per panel must be attached to the fuselage. A maximum prime power of 25 KVA can be provided by the C130 for the radar system.

B. *Wavelength selection.*

The wavelength for an airborne radar system is primarily defined by spatial resolution, along-track resolution, radar sensitivity, atmospheric attenuation, and cost. The NCAR airborne radar system requires sampling data density of 0.3 km out to a range of 10 km [2]. Resolution higher than 0.3 km requires radar with an antenna beamwidth less than 2° scanning with angular space less than 1° to produces moderately uncorrelated adjacent samples [3]. For airborne applications X-band was preferred because a narrow beamwidth can provides twice the spatial resolution of C-band and three times the spatial resolution of S-band. Table 1 presents a summary of the options under evaluation.

TABLE 1. TRADE-OFF ANALYSIS FOR X-, C-, AND S-BAND RADAR SYSTEMS.

Parameter	Units	Eldora	X-band	C-band	S-band
Frequency	GHz	9.4	9.4	5.4	2.4
Lambda	cm	3.2	3.2	5.5	9.3
# Elements (El/Az)	deg		118/110	64/56	40/34
# Total elements per panel	-		12,900	3,584	1,360
Beamwidth (El/Az)	deg	0.8/1.0	0.8/1.0	1.6/1.8	2.6/3.0
Equivalent time for independence	ms	6.4	6.4	11.1	20.0
Spatial resolution at 10km	m	314	174	314	523
Along-track resolution (continuous scanning)	m	300	300	400	760
Along-track resolution (beam multiplexing)	m	300	40	40	40

TABLE 2. SYSTEM CHARACTERISTICS AND COMPARISON WITH ELDORA SYSTEM.

Parameter	Units	Eldora (X-band)	APAR(C-band)
Frequency	GHz	9.3- 9.8	5.4
Wavelength	cm	3.22-3.06	5.5
# Elements (El/Az)	-	66	64/56
# Total elements per panel	-	-	3,584
Beamwidth (El/Az)	deg	0.8/1.0	1.6/1.8
Antenna gain	dB	40	41
Min. detect. signal at 10 Km	dBZ	-19	-15
Sildelobe level	dB	-20 to -24	-25
Pulse repletion frequency	Hz	2000	2000
Peak transmit power	Kw	36-50	14.3
Spatial resolution at 10km	m	314	314
Along-track resolution	m	300	40 (*)
Pulse width	us	0.1-3.0	0.5-50
Polarization	-	Horizontal	Dual Linear
Beam overlapping	%	35	35
Unambiguous range	km	20	75
Unambiguous velocity	m/s	13	50
Transmitted waveform	-	Phase-code PC Pulse compression	Pulse compression (PC)

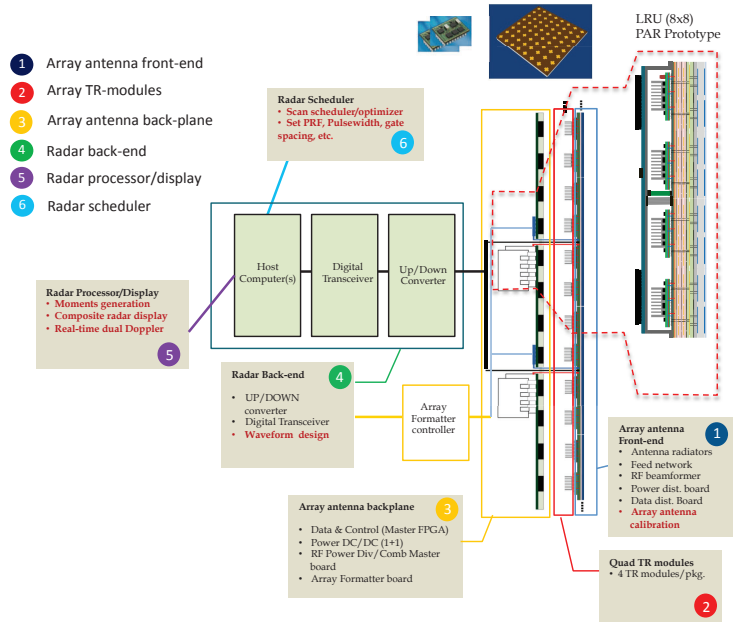

Fig. 3. Simplified block diagram of APAR. Subsystems 1-3 reside outside the fuselage enclosed by fairings and the rest of the system resides inside the cabin.

Antenna beamwidth also affect the spatial sampling in the along-flight track direction. The along-track resolution is proportional to the scanning rate and speed of the aircraft. The time required for a scan of a specific volume depends of the scanning strategy adopted in the radar system. When using phased array technology, the time to sample an entire volume can be less than 15 seconds. The scanning time depends on the antenna beamwidth, number of beams, beam overlapping, pulse repetition frequency, and number of pulses. When the phased array is used for a continuous scan mode (the case with the mechanical scan radars) the scanning rate is determined by the time it takes to obtain independent samples. Time to independence is estimated using the expression (3.18) in [10]. It is proportional to the wavelength and inversely proportionally to the accuracy of the radar velocity. Using this expression for different frequencies and an accuracy velocity of 1.0 m/s, X-band requires 6.4 ms to get independent samples, while C-band and S-band require 11.1 ms and 20 ms, respectively.

Along-track resolution as a function of the independent samples is illustrated in Figure 4. The dashed lines represent the along-track resolution as a function of independent samples for continuous scan mode. Considering ten independent samples and a flight speed of 120 m/s, scanning range of 90 °, beam overlap of 35%, and pulse repetition frequency of 2000 Hz., the along-track resolution is 350 m for X-band, about 430 m for C-band, and 800 m for S-band. In order to improve the current resolution to exceed the ELDORA along-track resolution of 300 m., phased array radar requires a spatial beam multiplexing scanning technique [4]. A beam multiplexing scanning technique takes advantage of the fast and flexible electronic scan to point the antenna beam pattern in any arbitrary position. In this mode the scanning rate is not limited by the de-correlation time. Figure 4 illustrates the along-track resolution using the beam multiplexing technique. Considering ten independent samples, the along-track resolution is below 200 m for the three bands (X-, C-, and S-band). In contrast to the continuous scanning mode, in the beam-multiplexing mode, the along-track resolution is worse for higher frequencies.

The accuracy of the radar's mean velocity measurements is related to the number of independent samples, turbulence intensity, radar wavelength, the unambiguous velocity, and the signal-to-noise ratio [10]. For distributed weather targets, accurate radar measurements (<2 m/s) require averaging a number of samples to produce mean values with the necessary accuracy. Velocity variance due to the number of independent samples and signal-to-noise ratio can be expressed using equation (11) in [10]. Figure 5 illustrates the number of independent samples required as a function of the SNR for a 1m/s accuracy mean velocity.

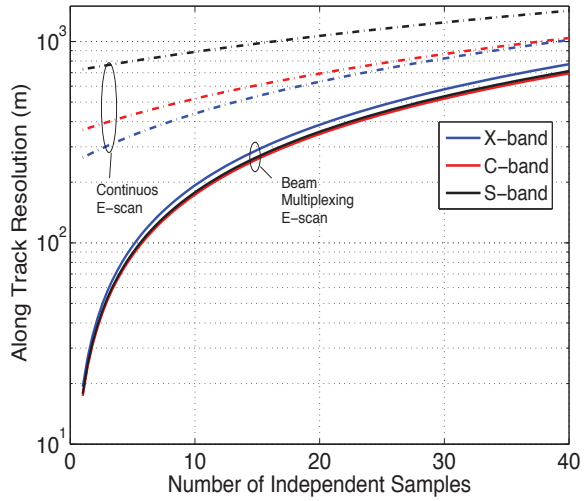

Fig. 4. Along-track resolution as a function of the number of independent samples for S-band, C-band, and X-band. Scanning range of 90º, beam overlapped factor of 35 %, flight speed of 120 m/s, and PRF of 2000Hz,

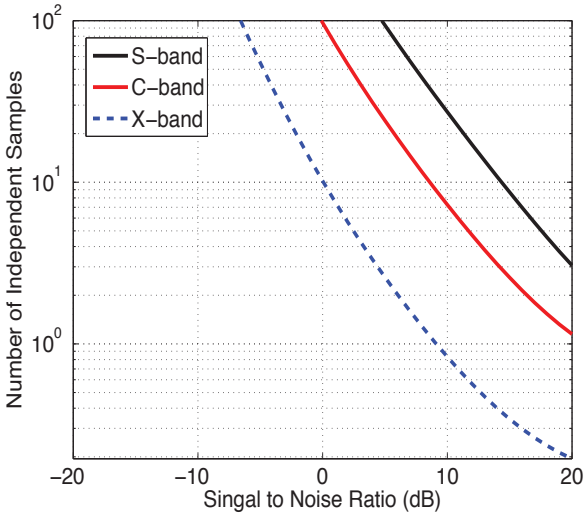

Fig. 5. Number of independent samples versus signal-to-noise ratio for S-band, C-band and X-band. All calculated for mean velocity measurement accuracy of 1 m/s and a PRF of 2000Hz.

For 10 independent samples, an X-band radar requires a *SNR* of 0 dB while C-band requires 9 dB and S-band requires 15 dB, respectively.

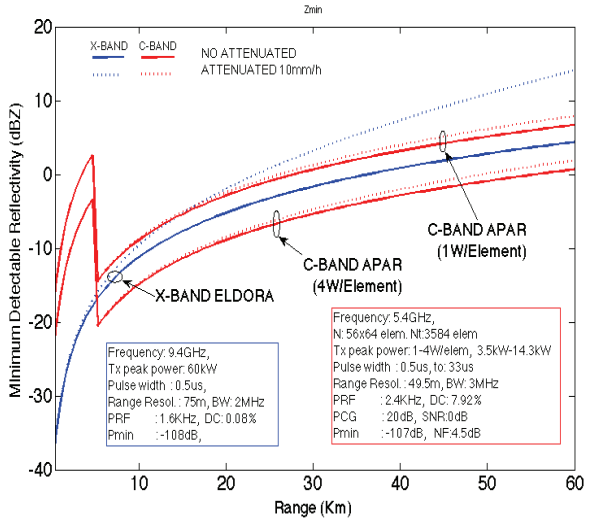

Fig. 6. Number of independent samples versus signal-to-noise ratio for S-band, C-band, and X-band, all calculated for a mean velocity measurement accuracy of 1m/s, and PRF=2000 Hz.

C. *Transmit power and radar sensitivity*

The proposed airborne phased array radar (APAR) will estimate dynamic and microphysical observations of clouds and precipitation in conjunction with in situ sampling of the same. Various technical specifications of the APAR radar were investigated by varying the number of radiating elements and peak power. Another important aspect that involves the selection of wavelength is the adversity of attenuation of the atmospheric gases and also by the hydrometeors. Commercial solid state T/R modules at C-band have been identified that can transmit either 1 W or 4 W peak power. Solid state T/R modules are capable of transmitting long pulses for significantly improving average transmit power. They can transmit variable pulse lengths between 0.5 and 50 μs. In the case of a 1 W T/R module with 1 μs pulse width, the total peak transmit power is 3.6 kW. Radar sensitivity is linearly proportional to the peak transmit power. As shown in Figure 6, sensitivity of the 4 W T/R element is better than the 1 W T/R element by 6 dB. But the 4 W T/R module does not meet the requirement of -12 dBZ sensitivity at 10 km. By transmitting 33 μs pulse, 4 W T/R modules, and using a pulse compression scheme, the sensitivity is improved to -27 dBZ at 10 km.

The long pulse of 33 μs creates a blind zone of 5 km around the aircraft. The blind zone can be eliminated by transmitting an intermittent short pulse of 1 μs. Transmission of short and long pulses leads to abrupt changes in sensitivity at a 5 km range. Since at a range less than 5 km radar detects better than -10 dBZ, the abrupt change in sensitivity due to long and short pulses will have no impact on detecting a precipitation echo.

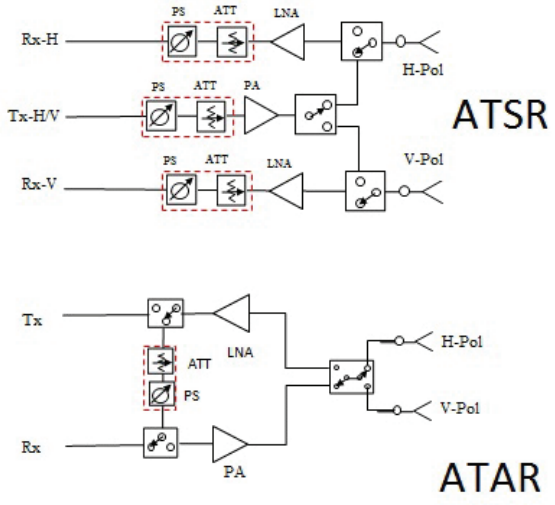

Fig. 7 Simplified block diagram of T/R modules for ATSR and ATAR polarization mode.

D. *Linear dual polarization and T/R modules.*

Two important requirements for dual-polarized antenna radar should be satisfied to provide errors less than 0.2 dB in differential reflectivity (Z_{dr}) when an alternate transmit mode is required. The first requirement is that the mismatch between antenna patterns (H and V) over the scan volume should not exceed 5% integrated power over the main beam. The second requires that the cross-polarization isolation between the H and V patterns should be less than -20 dB across the scan volume. Mismatch of the antenna patterns in a phased array antenna is larger than in a dish antenna. The mutual coupling, surface waves, and diffracted fields at the edges of the LRU array antennas are the principal causes of mismatch in the phased array antennas. Achieving the isolation level required (below -25 dB) is easy in the E-plane and H-plane. Cross-coupling between polarization increases significantly in the D-plane. Achieving a cross-polarization isolation below -25 dB in the D-plane remains one of the most difficult challenges for antenna engineers. New antenna element designs with new features that help to suppress the higher field modes that degrade the cross-polarization are required for accurate weather phased array radars. In next section, preliminary results of a new radiating antenna element that satisfies both requirements are presented.

Figure 7 illustrates the two basic architectures of the dual-polarized T/R modules for ATAR and ATSR. Complexity, number of components, calibration complexity, reliability, and cost can differ significantly for these two configurations. In comparison with ATSR, ATAR provides a simple architecture that reduces the number of components. Fewer elements relax the space constrains, improve dissipation of power, facilitate the calibration procedure, reduce the costs, and improve the failure rate.

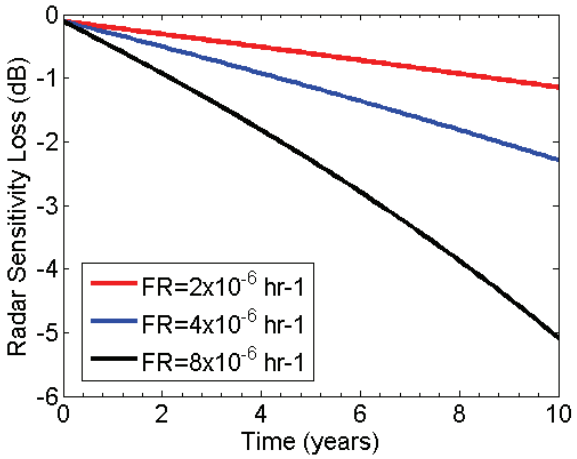

Fig. 8. Radar sensitivity loss versus time for different failure rate of TR Module.

E. Graceful degradation

Another important benefit of using phased array antenna technology is its higher reliability performance. An active electronically scanned arrays (AESA) is typically composed of a few thousand active elements, where each one provides transmit and receive functionality with independent low failures rates. Phased array antennas are very complex systems composed of several subsystems (antenna, T\R modules, backplanes, power supplies, formatter, etc). Each subsystem has different components and functionality; as a consequence, the failure rate of each subsystem is different. Passive components (aperture antenna board, RF beamformer, transmission lines, etc.) provide the lowest failure rates. Digital components such as FPGA, memories, and logic devices typically provide very low failure rates [15], [16]. Active components such as power amplifier, LNAs, regulators, and phase-shifters are typically the components in the AESA that have the highest failure rates. Typical failure rates of active T\R modules are estimated at between 2 to 8 failures per million hours of operation [17]. The failure rate is not the same for transmission and reception. Radar duty cycle and temperature conditions can significantly change the failure rate for the transmit and receive paths. Currently, RF companies have improved considerably the reliability characteristics of RF components: LNAs and phase shifters can be obtained with a failure rate below 0.1 $x10^{-6}$ hr^{-1}. CASA has developed a dual-pol, phased array radar using the ATAR T\R module. About 2.5 $x10^{-6}$ hr^{-1} is the estimated overall failure rate of each TR module [9].

Figure 8 illustrates the radar sensitivity losses versus operational time of PAR composed of one AESA of 3,853 elements in three T\R module failure rate scenarios. For these calculations we assume the system operate at a normal room temperature and the radar duty cycle is about 10%. Assuming the radar requires calibration after it reaches a radar sensitivity below -2 dB, T\R modules with a failure rate of 8 $x10^{-6}$ hr^{-1} can provide a continuous operation for up to 4 years. However, by reducing the failure rate of each T\R module in half (4 $x10^{-6}$ hr^{-1}), the radar operation time can be extended to 8 years.

D. Technology and cost

Between 50% and 60% of the overall cost of an AESA panel can be attributed to the T/R modules. The cost of T/R modules can vary based on operational frequency, polarization mode, technology, functionality, and volume. A short wavelength requires a more compact design that demands high component integration, which can be an issue for thermal dissipation and achieving high RF isolation. Currently multi-chip modules in X-band can be found on the market for $300 per unit. CASA X-Band T\R modules cost $567 (for 100 units), which can be reduced to $341 if large quantities (>1000 units) are produced [9]. The estimated cost of a C-band ATSR T\R module based on COTS components is $399 and it can be reduced to $188 for a production volume of 10,000 units. Figure 9 shows the cost breakdown percentage for an AESA using ATSR for a production volume of 10,000 units.

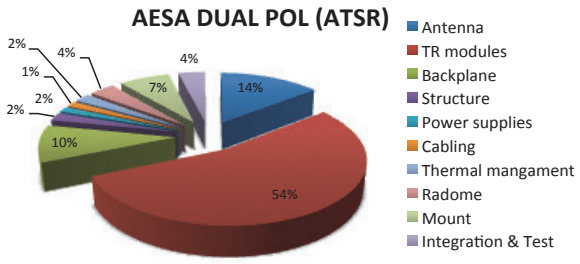

Fig. 9. Breakdown cost percentage for AESA using COTS component in ATSR polarization for a production volume of 10,000 units.

Polarization and functionality can also increase the cost of the system. Based on current COTS components, a C-band ATSR T\R module is 30% more expensive than an ATAR due to the two additional channels required.

IV. Preliminary Design

A. LRU architecture

The LRU architecture is defined in four parts, as illustrated in Figure 10(c). The first part is the aperture antenna board and it is composed of radome, antenna radiating elements, and RF distribution for H and V polarization and a power/data distribution board. The second part is composed of the T/R modules and heat sinks. The third part consists of a metal frame that provides support and canalizes air flow for thermal dissipation.

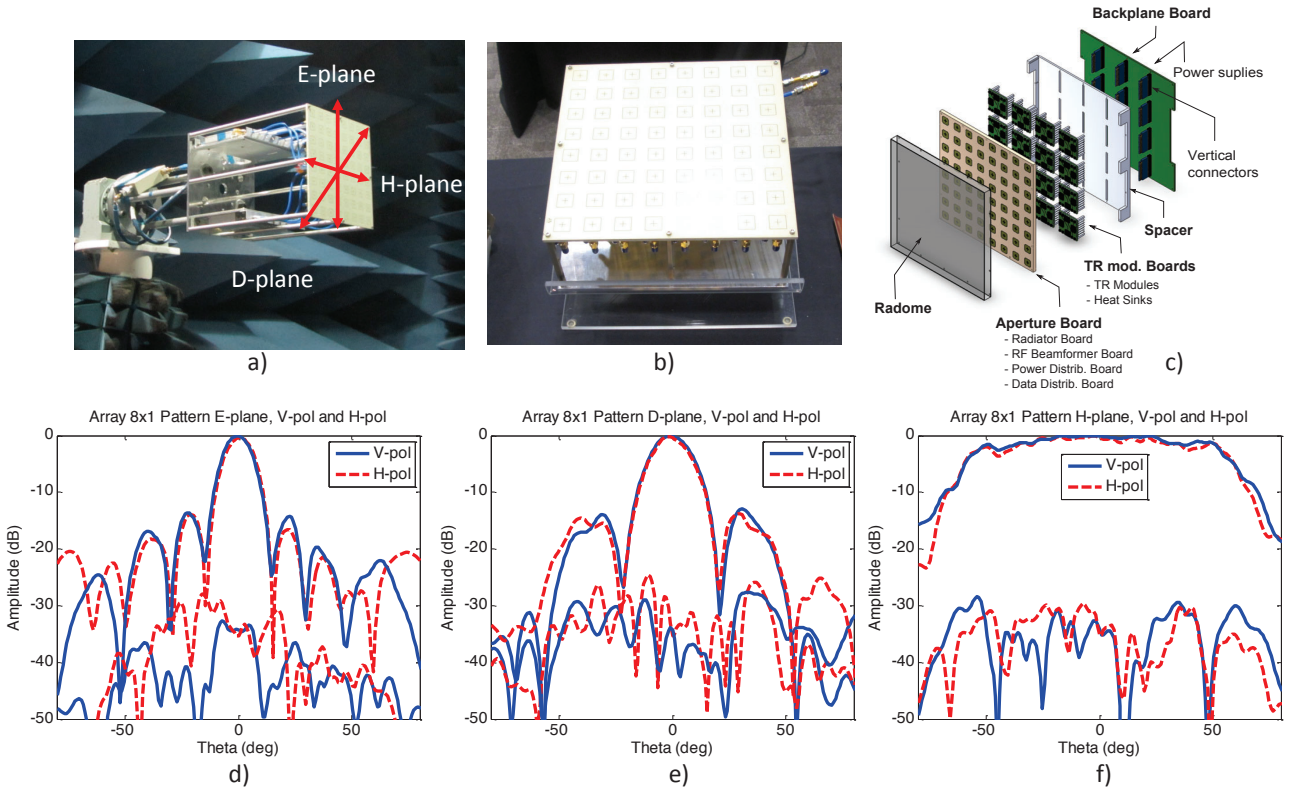

Fig. 10. LRU array antenna. a) LRU array antenna in first RF anechoic chamber. b) LRU aperture antenna board. c) AESA LRU architecture. d) Antenna patterns for 8x1 array, co-, and cross-pol for H and V in E-plane. e) Antenna patterns for 8x1 array, co- and cross-pol for H and V in D-plane. f) Antenna patterns for 8x1 array, co- and cross-pol for H and V in H-plane.

The fourth part is the backplane. This board provides the power conditioning and interfaces with the radar back end board to provide functionality and power to the LRU panel.

B. Radiating Aperture board design.

The radiating antenna LRU array is composed of 8x8 elements configured in a square lattice with a spacing element of half a lambda. A new dual-polarized radiating element was designed to provide a minimum mismatch between co-polar antenna patterns, maximum port isolation, and maximum cross-polarization, especially in the D-plane. A careful design was performed to minimize the surfaces waves and spurious radiation.

C. LRU radiating aperture board measured Results.

The LRU antenna array (8x8 elements) was prototyped and tested. Scattering parameters (return loss and isolation) for each element in the array in the E-, H-, and D-planes using an Agilent Network analyser were measured.

A return loss below -20 dB has been obtained for both polarizations at 5.4 GHz. An impedance bandwidth of 340 MHz at -10dB return loss is reported. Isolation better than -40 dB between the H and V ports was obtained. The first RF planar NSI near-field system was used to obtain the antenna patterns. The embedded element pattern in the LRU antenna aperture and also the linear array pattern of 8x1 elements in the H-plane were measured. Figure 10 d), e), and f) show the measured antenna patterns for H and V polarization at the center frequency (5.4 GHz) for E (ϕ =0 ^{o}), H (ϕ =90 ^{o}), and D plane (ϕ =45 ^{o}). Figure 10 d) illustrates antenna patterns for 8x1 array, co-, and cross-pol for H and V in E-plane. A cross-polarization below -30 dB is obtained. Figure 10 e) illustrates antenna patterns for 8x1 array, co-, and cross-pol for H and V in D-plane. Cross-polarization below -25 dB were obtained. Figure 10 f) illustrates antenna patterns for 8x1 array, co-, and cross-pol for H and V in H-plane. Cross-polarizations below -28 dB were obtained.

IV Summary

APAR with dual-polarization and dual-Doppler capability (greatly improved from ELDORA) allows microphysical (e.g., precipitation types and sizes, quantitative precipitation estimation) and 3-D wind estimation in a precipitation system. Multiple AESA radars on a C-130 fuselage enhance spatial and temporal resolutions of measurements. Multiple options (S-, C-, and X-band) have been evaluated, and a trade-off between wavelength, sampling, sensitivity, cost, and resolution has been considered in order to define the APAR architecture. C-band APAR is the architecture selected for the NCAR APAR system. A design of the APAR architecture based on ATSR polarization modes was initiated. Preliminary results of the antenna LRU aperture board demonstrate the possibility of performing dual-polarization radar for 2D scanning planar AESA.

Acknowledgments

This material is based upon work supported by the National Science Foundation under Grant Number (M0904552). Any opinions, findings, and conclusions or recommendations expressed in this material are those of the author(s) and do not necessarily reflect the views of the National Science Foundation. The authors also would like to acknowledge Keith Kelly from First RF Corporation for facilitating the anechoic chamber for the antenna LRU array antenna measurements. We also would like to thanks to Alessio Mancini for collaborate in the antenna LRU testing.

References

[1] Loew, E., W. Lee, J. Vivekanandan, J. A. Moore, J. S. Heard, and S. M. Duffy, 2007: An Airborne Phased Array Radar Concept for Atmospheric Research. 33rd Conf. on Radar Meteor, 6-10 August 2007.

[2] Wen Chau Lee, Jothiram Vivekanandan, Eric Loew and Jorge L. Salazar, 2013: A Dual-Polarized, Airborne Phased Array Radar for Atmospheric Research. 36 th Conf. on Radar Meteor, 16-20 September 2013.

[3] P. H Hildebrand, W. C. Lee, C. A. Walther, C. Frush, M. Randall, E. Loew, R. Neitzel, R. Parsons, J. Testud, F. Baudin, and A. LeCornec, 1996: The ELDORA/ASTRAIA airborne Doppler weather radar design and observations from TOGA COARE, Bull. Amer. Meteor. Soc., vol 77, pp. 213-232, 1996.

[4] Heinselman, Pamela L., Sebastián M. Torres, 2011: High-Temporal-Resolution Capabilities of the National Weather Radar Testbed Phased-Array Radar. J. Appl. Meteor. Climatol., 50, 579–593.

[5] M.M. French, I. PopStefanija, R.T. Bluth, and J.B. Knorr, 2010: A mobile, phased-array Doppler radar for the study of severe convective storms. Bull. Amer. Meteor. Soc., 91, 579-600.

[6] Weber, Mark E., John Y. N. Cho, Jeffrey S. Herd, James M. Flavin, William E. Benner, Garth S. Torok, 2007: The Next-Generation Multimission U.S. Surveillance Radar Network. Bull. Amer. Meteor. Soc., 88, 1739–1751.

[7] G. Zhang, R. J. Doviak, D. S. Zrnic, J. E. Crain, D. Staiman, and Y. Al-Rashid, 2009: Phased array radar polarimetry for weather sensing: a theoretical formulation for polarization calibration, IEEE Trans. on Geoscience and Remote Sensing, vol. 47(11), pp. 3679-3689, 2009.

[8] Zhang, Guifu, Richard J. Doviak, Dusan S. Zrnić, Robert Palmer, Lei Lei, Yasser Al-Rashid, 2011: Polarimetric Phased-Array Radar for Weather Measurement: A Planar or Cylindrical Configuration?. *J. Atmos. Oceanic Technol.*, **28**, 63–73.

[9] Jorge L. Salazar, 2011: Feasibility of Low-Cost Dual- Polarized, Phase-tilt Antenna Arrays for Dense Radar Networks, University of Massachusetts, Amherst, 2011.

[10] Freed E. Nathanson, 1990: Radar Design Principles, 2nd ed., McGraw-Hill, 1990.

[11] V. N. Bringi and V. Chandrasekar, 2001: Polarimetric Doppler Weather Radar: Principle and applications, Cambridge University Press, 2001

[12] Wang, Y., and V. Chandrasekar, 2006: Polarization isolation requirements for linear dual-polarization weather radar in simultaneous transmission mode of operation. IEEE Trans. Geosci. Remote Sens., 40, 2019–2028.

[13] J.L Salazar, R. H. Medina, E. Knapp and D. J. McLaughlin, 2012: Low-cost X-band Dual Polarized Phased Array Antenna Performance, European Microwave Week Conference, Amsterdam, Netherlands, October 2012.

[14] R. Medina, E. Knapp, J. Salazar, D. McLaughlin, T/R Module for CASA Phase-Tilt Radar Antenna Array, European Microwave Week Conference, Amsterdam, Netherlands, October 2012.

[15] Ashok K. Agrawal and Eric L. Holzman, "Active Phased Array Design for High Reliability", Transactions on Aerospace and Electronic Systems, Vol. 35, No. 4, October 1999

[16] MIL-Handbook 217: 1991.

[17] David N. Mcquiddy, Ronal L. Gassner, Porter Hull, James S. Mason and John M. Bendinger, 1991: Transmit/Receive Module Technology for X-band Active Array Radar. Proceeding of the IEEE, vol. 79, No. 3, March 1991.